Control and Operation of Dynamic Voltage Restorer With Online Regulated DC-Link Capacitor in Microgrid System

Contrôle et fonctionnement du restaurateur de tension dynamique avec condensateur de liaison CC en ligne régulé dans un système à microréseau

Tarek Kandil and Mohamed Adel Ahmed

***Abstract*— This article presents a dynamic voltage restorer (DVR) topology based on the adaptive noise canceling (ANC) technique, which can be used for both voltage compensation and harmonic mitigation. Furthermore, this article aims to investigate the DVR performance when installed in a microgrid (MG) during both normal operation of the utility and during utility disturbances. One of the main objectives of this article is to reduce the cost of inverter-based DVR by reducing both the size of the dc-link capacitor and rating of switching elements. The voltage of the dc-link capacitor is regulated to low voltage level using a transformer and a pulsewidth modulation (PWM) rectifier to achieve both effective voltage regulation and drawing a sinusoidal line current from the grid and thus not to contribute to the increase of the THD of the utility current. Furthermore, the voltage across the switches can be limited to low value by an adequate design of dc-link capacitor size, capacitor voltage, and sag level to be compensated. Finally, the effectiveness and fast response of the proposed DVR for the compensation of voltage disturbances and current harmonics is confirmed by simulation using MATLAB/Simulink during the steady-state and transient operations to analyze the performance of the scheme under different operating conditions.**

***Résumé*— Cet article présente une topologie de restauration de tension dynamique (DVR) basée sur la technique d'annulation adaptative de bruit (ANC), qui peut être utilisée à la fois pour la compensation de tension et l'atténuation des harmoniques. En outre, cet article vise à étudier les performances du DVR lorsqu'il est installé dans un microréseau (MG) pendant le fonctionnment normal de l'utilitaire et pendant les perturbations de l'utilitaire. L'un des principaux objectifs de cet article est de réduire le coût de l'onduleur DVR en réduisant à la fois la taille du condensateur de liaison cc et l'évaluation des éléments de commutation. La tension du condensateur de liaison cc est régulée à un niveau de tension faible à l'aide d'un transformateur et d'un redresseur à modulation de largeur d'impulsion (PWM) pour obtenir à la fois une régulation de tension efficace et produire un courant de ligne sinusoïdal à partir du réseau et donc pour éviter de contribuer à l'augmentation de la THD du courant de service. En outre, la tension aux bornes des commutateurs peut être limitée à une valeur faible par une conception adéquate de la taille du condensateur à liaison cc, de la tension du condensateur et du niveau d'affaissement à compenser. Enfin, l'efficacité et la réponse rapide du DVR proposé pour la compensation des perturbations de tension et des harmoniques de courant sont confirmées par une simulation utilisant MATLAB / Simulink pendant les opérations en régime permanent et transitoire pour analyser les performances du schéma dans différentes conditions de fonctionnement.**

***Index Terms*— Adaptive noise canceling (ANC), dynamic voltage restorer (DVR), harmonic mitigation, microgrid (MG), pulsewidth modulation (PWM) rectifier, voltage compensation.**

I. Introduction

MICROGRID (MG) is a way of integrating distributed generators into the electric network and therefore can be used to integrate various kinds of renewable energy resources that have got recently increasing attention in many countries, such as Saudi Arabia. For example, Saudi Arabia intended to produce over 50% of its electricity needs (or electric power generation) from solar and wind energies by the year 2030, which can be realized from the national Saudi Vision 2030 [1]. Furthermore, MGs have many benefits, such as supplying power locally and hence reducing energy losses and upstream congestion in transmission lines, increasing reliability, decreasing operation costs, reducing grid investment, and finally reducing loading of transmission and distribution, thereby deferring planned substation upgrades [2]–[4]. Besides, the demand for renewable energy sources in large urban cities is increasing, and their integration with the

Manuscript received January 12, 2020; revised March 30, 2020; accepted June 9, 2020. Date of current version October 27, 2020. This work was supported by Jouf University under research project (40/263). *(Corresponding author: Mohamed Adel Ahmed.)*

Tarek Kandil is with the Electrical Engineering Department, Jouf University, Sakakah 2014, Saudi Arabia, and also with the Electrical Engineering Department, Al-Azhar University, Cairo 11651, Egypt (e-mail: takandil@ju.edu.sa).

Mohamed Adel Ahmed is with the Electrical Engineering Department, Jouf University, Sakakah 2014, Saudi Arabia, and also with the Electrical Engineering Department, Benha University, Banha 13518, Egypt (e-mail: madel@ju.edu.sa).

Associate Editor managing this paper's review: Fabio Immovilli.

Digital Object Identifier 10.1109/CJECE.2020.3002855

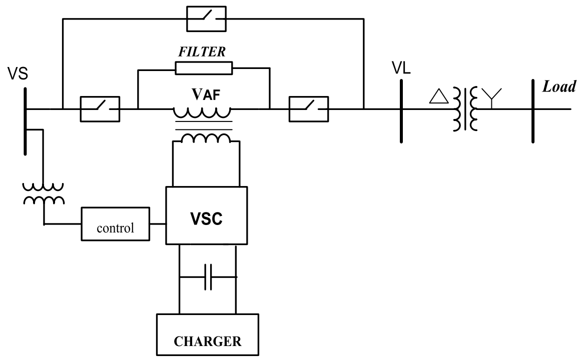

Fig. 1. DVR components and connection.

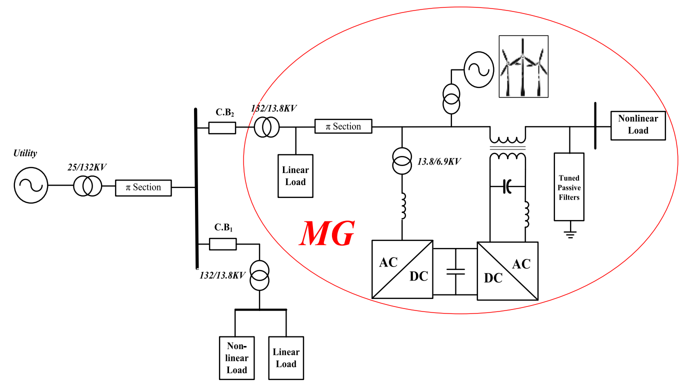

Fig. 2. Single line diagram of the simulated power system and MG.

existing conventional grid is essential. Therefore, the future requires more attention to insure having stable and reliable integration of MG to the utility grid and further stable and reliable MG when it is disconnected from the main grid and operated in stand-alone mode. However, there are some technical challenges facing MGs such as follows.

1) The wide usage of nonlinear loads produces harmonics that may interact with system impedances and lead to voltage harmonics. These voltage harmonics may badly affect sensitive loads and may be subjected to nuisance tripping of relays during these load variations [5], [6].
2) Frequent starting and shutdown operations of generators will lead to voltage fluctuations, especially sag that may cause huge economic losses when it exceeds even two or three cycles [7].
3) When MG is connected to the utility, at the distribution level, the voltage sags occur when a short-circuit fault takes place on a parallel feeder and large motor starting and transformer energizing, which may cause a transient increase in current and this will cause voltage sags on the line [8], [9].
4) Reliable operation of MG when it is working in stand-alone mode or if islanded from the main grid in response to abnormal conditions that the utility may experience.

Dynamic voltage restorer (DVR) is a device that can eliminate most voltage sags and minimize the risk of load tripping during sags so that the loads are insulated from power reliability issues [10], [11]. Furthermore, it can be used for harmonic mitigation [12]–[14] and unbalanced voltage compensation [15]–[18]. The main components of the DVR and its connection with the power system are shown in Fig. 1 [19]. The DVR consists of a dc power source, an inverter, an injection transformer, which is connected in series with the power line and the sensitive load, and a passive filter.

Batteries, supercapacitors, superconducting magnetic storage units, and flywheels can be used as the dc power sources. The first commercial DVR installation was in North America in the year 1996 on a 12.47-kV system located in Anderson, SC, USA [20]. Currently, there are many companies that are commercially producing DVRs and claim that they can mitigate sags up to 70% in depth and for long periods (up to 30 s) and can provide independent compensation per phase.

With rapid advances in solid-state technology, material science, rechargeable batteries, and supercapacitor, a reduced-rating and cost-effective voltage source converter (VSC) can be achieved with an adequate design and regulation of the dc-link capacitor as well as precise control strategy.

Furthermore, a thorough investigation of the commonly used control strategies for DVR schemes has been carried out to adopt one that can meet both voltage compensation and harmonic mitigation requirements and can be easily implemented. Synchronous reference frame theory [16], instantaneous reactive power theory (IRP) [21], and frequency-domain analysis [22] are commonly used control techniques; however, they are difficult to adjust and complex to implement [23]. Therefore, a detection technique that is based on adaptive noise canceling (ANC) is chosen for generating the reference harmonic current command required for harmonic mitigation for a given load [24], which is easy to adjust, implement, and has a fast and accurate dynamic response for the detection of the required command signals. Furthermore, it is very simple to build experimentally with a very few logical gates and does not need a complex microprocessor or microcontroller codes that make it very easy to maintain as well.

This article is organized to provide a complete description of system under study, including the utility and the MG. Then, the DVR components are described and designed. Finally, the control and performance of the proposed DVR under different control techniques are demonstrated and investigated to help in assessing its performance during critical conditions. Moreover, this article evaluates the impact of the presence of nonlinear loads sharing the same bus with the DVR on its performance. The effectiveness of the design of the dc-link capacitor's voltage regulation circuit is assessed, which enables the precise selection of the dc-link capacitor size to reduce the cost of the DVR. The results can be very useful for design and maintenance engineers to evaluate the reliability and robustness of a given microgrid system.

II. Description of System Under Study

Fig. 2 shows the single line diagram of the utility system and MG used in this article. The utility comprises a 25-kV, 50-Hz power station that is transmitted to the MG through a transmission system, which is operated at 132 kV and is connected with the MG and a linear load through a 132-/13.8-kV transformer. The MG is fed locally from a 20-MVA wind farm through a step-up 0.73-/13.8-kV transformer and is feeding the following loads.

1) *Load*$_1$*:* 15-MVA nonlinear load with a DVR.
2) *Load*$_2$*:* 7-MVA nonlinear load.
3) *Load*$_3$*:* 8-MVA linear load.

The design, ratings, and control strategy of all DVR components will be described in Section III.

III. DVR Design and Compensation Techniques

The DVR employs a voltage source inverter (VSI) that converts the dc voltage supplied by the dc-link capacitor into an ac voltage. This voltage is then injected into the main system by a series transformer that is mostly a step-up transformer, and therefore, the VSI has low voltage and high current ratings [25]. Hysteresis voltage and current control is adopted in this article for the generation of the switching signals of the VSI to be used for both voltage compensation and load current harmonics mitigation. Finally, an ac shunt passive filter should be installed in parallel with the DVR circuit to provide a path for all harmonic currents that are blocked by the DVR circuit. A detailed explanation of each component of the DVR is provided in the following.

A. Series Transformer

It is preferred to limit the use of the DVR to abnormal conditions, which needs either using a bypass switch for the transformer during normal condition or a transformer with special design to have a very low reactance that will have a small voltage drop across its terminals. Furthermore, the current rating of transformer depends on the load current at point of common coupling.

B. Energy-Storage Capacitor

The VSI requires an energy-storage capacitor to provide power to the load during voltage sags and short interruption. Its size can be reduced by controlling its voltage to be limited to a range of relatively low values at a certain level above the peak of the supply voltage, which can improve the VSI controllability and reduce its cost. One of the methods used to control the capacitor voltage is to connect the dc side of the DVR to a dc chopper that is fed from bridge diode rectifier [26]. However, this method has the disadvantage of distorting the line current drawn from the supply. In this article, the required power for the dc-link capacitor of the DVR is provided by a pulsewidth modulation (PWM) rectifier that is fed from the supply side, as shown in Fig. 3.

The main purpose of the PWM rectifier shown in Fig. 4 is to maintain the dc-link voltage of DVR at the required level while drawing a sinusoidal line current that in-phase with the source voltage to provide a unity power factor operation. Furthermore, the control of the PWM rectifier is based on an online compensation method in which a proportional–integral (PI) controller is used to regulate the dc-link voltage and phase-locked loop (PLL) is used to generate three sine waves with unity magnitude.

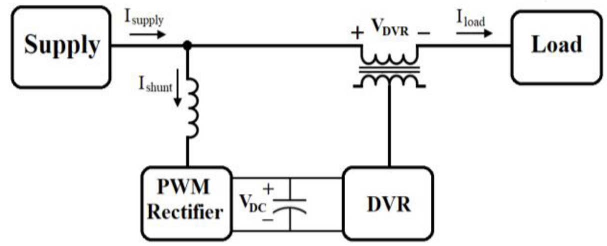

Fig. 3. DVR with PWM rectifier connected to the source side.

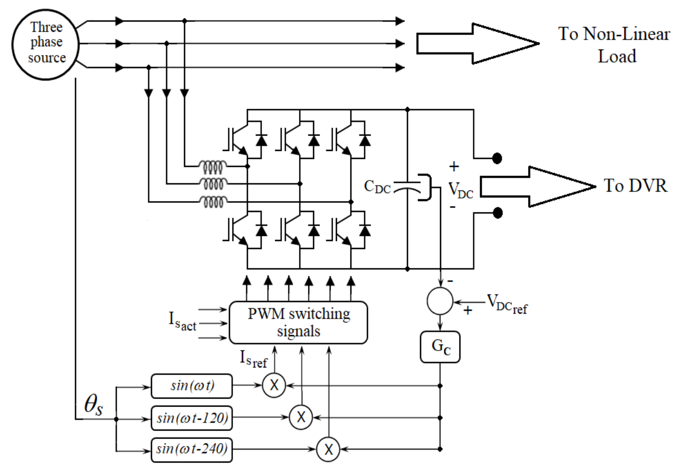

Fig. 4. PWM rectifier circuit details.

According to the principle of power balance, the output of PI controller is considered the peak value of line current. By multiplying the unity sin waves with PI controller output, a reference value of fundamental line current can be generated. A hysteresis current controller is then used to generate the switching signals required by the PWM rectifier.

To maintain a linear PWM operation and sinusoidal input currents, the dc-link voltage should be maintained as [27]

$$V_{\mathrm{dc}} \geq \frac{2\sqrt{2}}{\sqrt{3}} V_{\mathrm{LL}}. \tag{1}$$

Furthermore, the voltage ripple across the dc-link capacitor ΔV_{dc} should be precisely controlled to limit its size, which may contribute significantly to the VSI cost and can be modeled as [28]. For a given allowable peak ripple voltage of ΔV_{dc} and switching frequency, the minimum capacitor can be found as

$$C_{\min} = \frac{\sqrt{2} I_s + P_{\mathrm{out}}/V_{\mathrm{dc}}}{2\Delta V_{\mathrm{dc}} f_s}. \tag{2}$$

By relating the peak supply current to the output power, the capacitor value is

$$C_{\min} = P_{\mathrm{out}} \frac{\sqrt{2} + \sqrt{3} V_{\mathrm{LL}}/V_{\mathrm{dc}}}{2\sqrt{3}\Delta V_{\mathrm{dc}} f_s}. \tag{3}$$

C. Passive Filters

Two passive filters are required for the DVR scheme to work properly for both voltage compensation and harmonic mitigation. The first filter is a low-pass passive filter that should be installed at the VSI side of the boost transformer

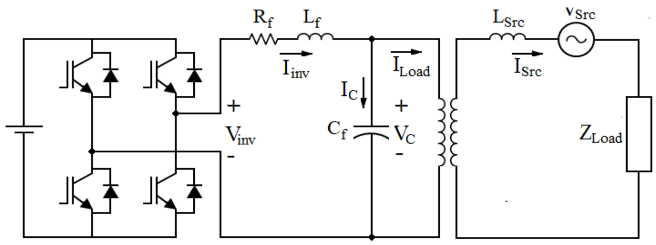

Fig. 5. Single-phase equivalent circuit of DVR.

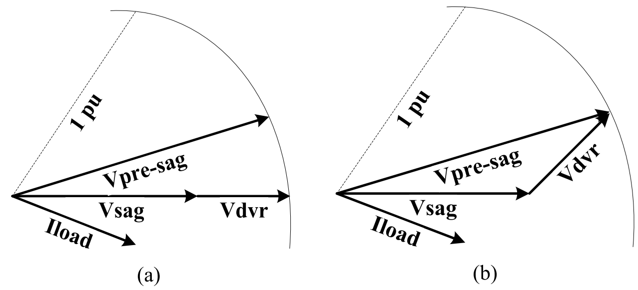

Fig. 6. Voltage compensation techniques of DVR. (a) In-phase compensation technique. (b) Pre-sag compensation technique.

to remove the unnecessary higher order harmonic components generated from the VSI and to prevent them from flowing through the boost transformer windings to decrease the distortion of the compensated output voltage and reduce the stress on the transformer [29]. The bandwidth of DVR is determined by carefully determining the cutoff frequency of the *LC* filter [30]. Fig. 5 shows the equivalent circuit of the DVR circuit, where V_{inv} is the output voltage of the inverter, L_f and C_f are the filter inductor and capacitor, respectively, and R_f is the series resistance of filter inductor and inverter switches.

According to Fig. 5, the transfer function of an *LC* filter can be derived as

$$\begin{aligned}\frac{V_{\text{Load}}}{V_{\text{inv}}} &= \frac{1/L_f C_f}{s^2 + sR_f/L_f + 1/L_f C_{f_s}}\\ &= \frac{\omega_f^2}{s^2 + 2\zeta_f \omega_f s + \omega_f^2}\\ \text{where, } \zeta_f &= \frac{R_f}{2}\sqrt{\frac{C_f}{L_f}}, \omega_f = \frac{1}{\sqrt{L_f C_{f_s}}}. \end{aligned} \tag{4}$$

For a given filter cutoff frequency ω_f, the filter inductance and capacitance can be determined.

The second passive filter should be installed in parallel with the DVR circuit to provide a path for all harmonic currents that are blocked by the DVR circuit. It should be tuned according to the expected harmonics generated by the load to provide a path for these currents. Mostly, three single tuned passive filters are employed to mitigate the fifth-, seventh-, and high-order harmonics. First, the capacitor of the filter should be designed to improve the system power factor, and then, the filter inductance is designed according to the following harmonic order required to be canceled. For example, the inductance of the fifth-harmonic filter is as follows:

$$L_{5\text{th}} = 1/\omega_n^2 \times C_{5\text{th}}. \tag{5}$$

D. Control Methodology of the DVR

The compensation is achieved by supplying or absorbing the real power and reactive power to or from the DVR. There are several voltage compensation techniques which have been discussed in the literature, including pre-sag voltage compensation technique, in-phase voltage compensation technique, and minimum energy technique [19], [31], [32]. A comparison between the "pre-sag" and "in-phase" voltage compensation technique, shown in Fig. 6, is carried to evaluate the performance of the DVR operation under these techniques for different loading conditions.

Furthermore, the harmonic mitigation is achieved by blocking the harmonic currents from flowing from the load to the mains by generating a harmonic voltage V_{dvr}^h equal to the harmonic voltage drop V_f^h at the shunt passive filter. The shunt passive filter is tuned to provide a path for all harmonic currents that are blocked by the DVR circuit. The ANC technique [24] is used to extract the harmonic component of the load current harmonics to achieve the harmonic mitigation as follows.

If the voltage at the point of common coupling $u_{\text{pcc}(t)}$ is assumed to be sinusoidal, then the load current $i_{L(t)}$ can be decomposed into three main components: active current component $i_{Lp(t)}$, reactive current component $i_{Lq(t)}$, and harmonic current $i_{Lh(t)}$ as follows:

$$i_{L(t)} = I_{Lp(t)} + I_{Lq(t)} + I_{Lh(t)} \tag{6}$$

where

$$\begin{aligned} I_{Lp(t)} &= I_1 \cos\theta_1 \sin\omega t\\ I_{Lq(t)} &= I_1 \sin\theta_1 \cos\omega t\\ I_{Lh(t)} &= \sum_{n=2}^{\infty} I_n \sin(n\omega t + \theta_n). \end{aligned}$$

The load instantaneous power can be derived based on the preceding information as

$$\begin{aligned} P_{L(t)} &= v_{\text{pcc}(t)} i_{L(t)}\\ P_{L(t)} &= V_m I_1 \cos\theta_1 \sin^2\omega t + V_m I_1 \sin\theta_1 \sin\omega t \cos\omega t\\ &\quad + \sum_{n=2}^{\infty} I_n \sin(n\omega t + \theta_n). \end{aligned} \tag{7}$$

The load average power can be then calculated by integrating (7)

$$P_{Lav} = \frac{1}{T}\int_0^t P_{L(t)} dt. \tag{8}$$

The final output of the integration process of (8) is given in (9) when applying the orthogonal function theory [23]

$$P_{Lav} = V_m I_1 \cos\theta_1. \tag{9}$$

The result of (9) equals to the peak value of the fundamental active current $i_{Lp}(t)$ in (6) when it is divided by a factor of V_m. This is done automatically by the ANC filter.

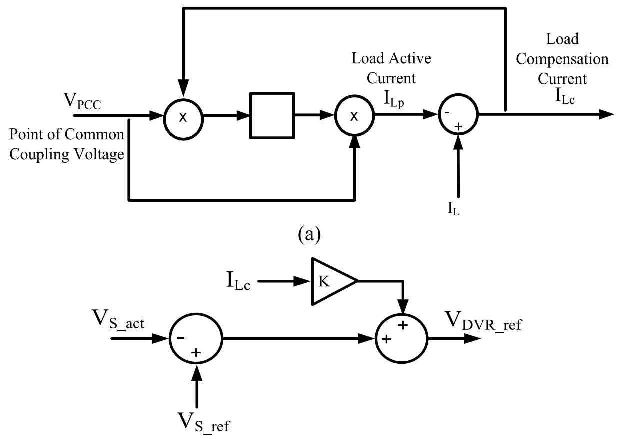

Fig. 7. Full control circuit for DVR. (a) Reference current generation. (b) Reference voltage generation.

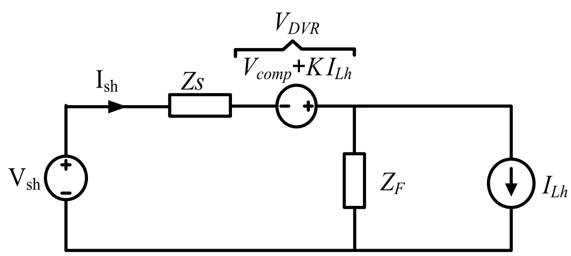

Fig. 8. Equivalent circuit of the DVR compensation scheme.

Finally, the harmonic mitigation command current $i_{c(t)}$ can then be extracted as follows:

$$i_{Lc(t)} = I_{L(t)} - I_{Lp(t)} = I_{Lq(t)} + I_{Lh(t)}. \tag{10}$$

To achieve the harmonic isolation, the DVR should inject a voltage that is proportional to the load compensation currents as in (10) as

$$V_{\mathrm{DVR}} = K \times I_{Lc} = K(I_{Lq} + I_{Lh}). \tag{11}$$

The full control circuit for generating the reference command voltage for the DVR $V_{\mathrm{DVR\_ref}(t)}$, which performs the previous procedure and achieves both voltage compensation and harmonic mitigation, is shown in Fig. 7.

Neglecting the effect of the compensation voltage of the DVR (V_{comp}), the supply current harmonics I_{sh}, is obtained from the equivalent circuit, shown in Fig. 8, as

$$I_{\mathrm{sh}} = I_{Lh}\frac{Z_F}{Z_S + Z_F + K} + V_{\mathrm{sh}}\frac{1}{Z_S + Z_F + K}. \tag{12}$$

From (7), the supply current harmonics i_{sh} depends on the gain (K). If the gain is selected so that $K \gg Z_S Z_F$, the load current harmonics will be isolated from the supply.

IV. Modeling and SimulatION of the SyStem Under Study

The power system described in Fig. 2 has been modeled by MATLAB/Simulink to evaluate the performance of the designed DVR when operated inside the MG. A complete model of the utility system, MG, and the designed DVR circuit

TABLE I
Simulation Parameters of the System

Microgrid parameters	Bus-voltage	13.8 kV
	Wind-farm	730 V, 50 MVA
	Wind-farm transformer	50 MVA, 0.73/13.8kV
	Load 1	30 MVA linear inductive load
	Load 2	12 MVA non-linear load with DVR
DVR parameters	DC- link voltage	Max. 10 kV, Min. 5 kV
	DC- link capacitor	Max. 5000 μF, Min. 2000 μF
	Injection transformer	1MVA, 10 kV, a=1:1
	Filter inductor, L_f	2.4 mH
	Filter capacitor, C_f	52 μF
PWM rectifier parameters	DC- link voltage	Max. 10 kV, Min. 5 kV
	Coupling transformer	5 MVA, 13.8/6.9 kV
	Line inductor L	7.5 mH
	DC- link capacitor, C	Max. 5000 μF, Min. 2000 μF
	DC-voltage PI controller	Kp=0.8, ki=1.5
Shunt passive filters	5^{th} harmonic filter	L= 156 mH, C= 2.6 μF
	7^{th} harmonic filter	L= 0.08 H, C= 2.6 μF
	Higher order harmonic filter	L= 5 mH, C= 80 μF, R= 5 Ω

described in Section III is shown in Fig. 9. The following DVR parameters are used.

1) The DVR has a dc-link capacitor that is regulated for a 10 000 V_{dc}.
2) The VSI has a low-pass filter installed in the injection transformer side, which is selected to have a 52 μF and 2.4 mH to have a cutoff frequency of 450 Hz.
3) The turns ratio of the three single-phase injection transformers is (1:1) and their rated power is 5 MVA.
4) The shunt passive filter is tuned to fifth-, seventh-, and high-order harmonics of load. The parameters of the shunt passive filter are 2.6 μF and 0.156 H, for fifth harmonic and 2.6 μF and 0.08 H for seventh harmonic.
5) The MG's nonlinear load is a three-phase bridge rectifier with a resistive load that has a rating of 12 MVA.

The simulation parameters of the proposed DVR-microgrid system are shown in Table I.

The validity of the DVR design is examined for two modes of operation of the described system, which are given in the following.

Mode I: Normal operating conditions of the MG when it is connected with the utility to supply both the utility and MG loads and there is no disturbance in the system.

Mode II: Abnormal operating conditions of the MG when it is connected with the utility to supply both the utility and MG loads and there are successive disturbances in the system.

A. Mode I: Normal Operating Conditions of MG

During this mode, the only voltage drop in the system is due to the losses in the utility transmission line, 30 km. The waveforms shown in Figs. 10–12 are for Phase-A of the system when using the "in-phase" control technique. Fig. 10 shows

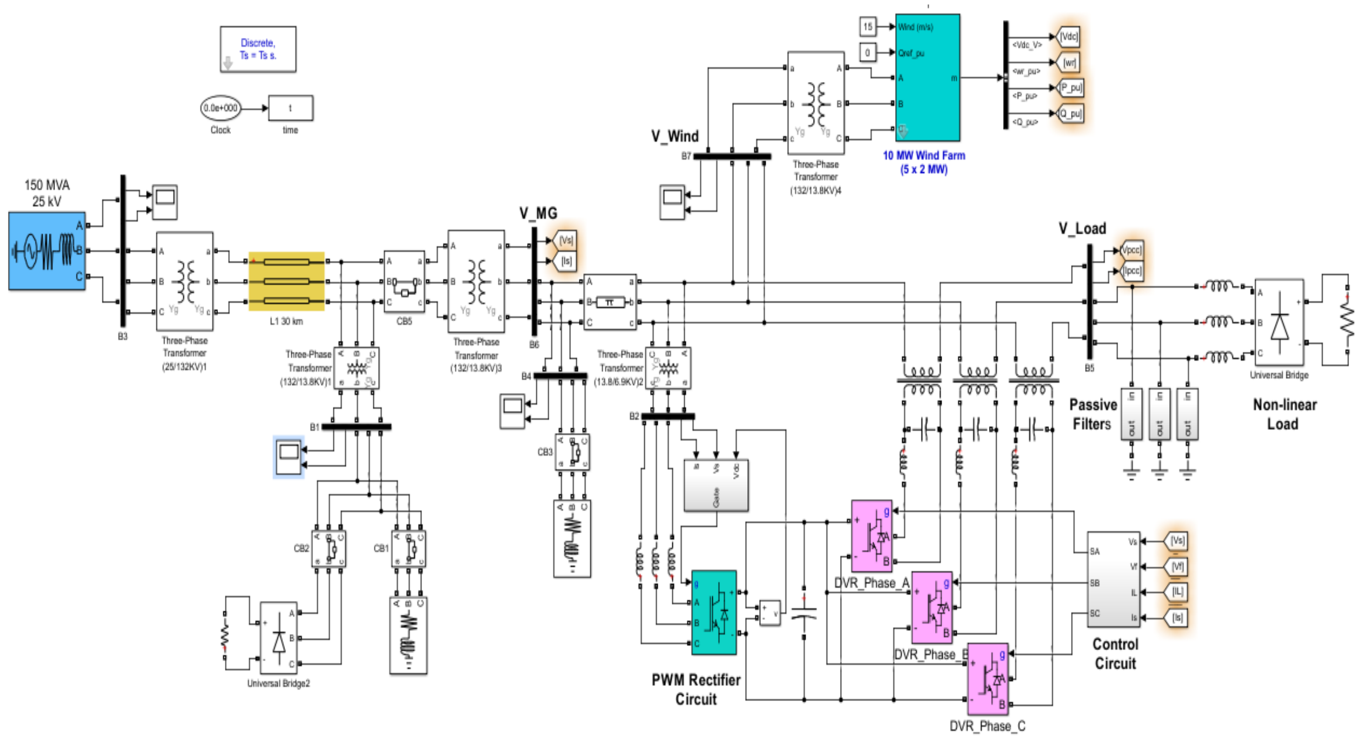

Fig. 9. Complete model of the simulated system using MATLAB/Simulink.

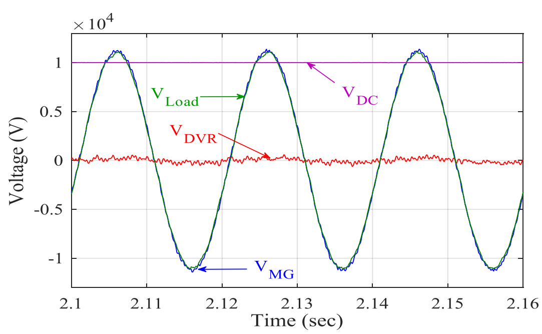

Fig. 10. MG front-end voltage V_{MG}, DVR voltage V_{DVR}, load voltage V_{Load}, and dc-link capacitor voltage V_{dc}.

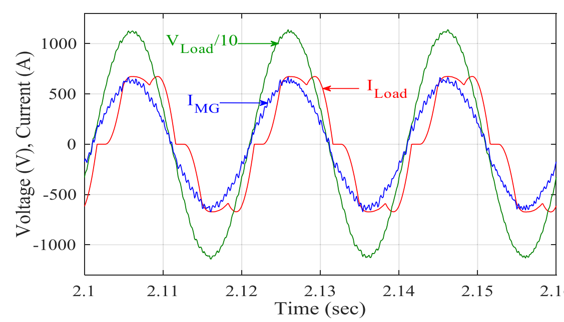

Fig. 11. Load voltage, load current, and source current during normal operation using the in-phase control technique.

the voltage at the front end of the MG V_{MG}, the DVR voltage V_{DVR}, the load voltage V_{Load}, and the capacitor voltage V_{dc}. As the voltage drop in the transmission line is expected to be compensated by the utility before reaching the MG by both increasing the plant output voltage and installing shunt capacitors, the MG front-end voltage level is expected to be very close to the reference voltage that has the same phase of V_{MG}. Thus, the DVR voltage is very close to zero level and only compensates for the voltage drop of the series boosting transformer of the DVR, as shown in Fig. 11, and thus, V_{MG} is equal to V_{Load}. Furthermore, as the DVR is injecting a voltage that is proportional to both load reactive and harmonic currents, it could improve power factor to almost unity, as shown in Fig. 11.

The DVR harmonic's blocking capability could limit the load current's harmonics by decreasing its THD from 16.88% to 5.65% as can be observed from harmonic spectrum shown in Fig. 12 and the measured values in Table II.

TABLE II
IMPORTANT PARAMETER MAGNITUDES AND THD DURING THE NORMAL OPERATION

Parameter	V_{MG} (V)	V_{DVR} (V)	V_L (V)	I_L (%THD)	I_{MG} (%THD)
Value	7910	205	8115	16.88	5.65

It is worth mentioning that the harmonic blocking capability depends on the control circuit gain (K) mentioned in (11). Therefore, an investigation of the effect of this gain on the percentage change of load current THD is carried out to have a complete understanding of its overall effect on the circuit performance, as shown in Fig. 13. Fig. 13 reveals that the THD decreases sharply with the increase of the gain (K) and saturates when approaching the load impedance. Furthermore, it can be concluded that the voltage injected V_{dvr}^{h} mentioned in (11) is very small compared with the MG line voltage,

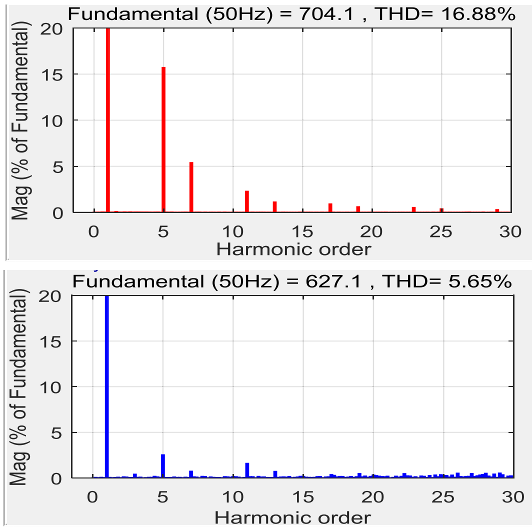

Fig. 12. Harmonic spectrum of (a) load current and (b) source current.

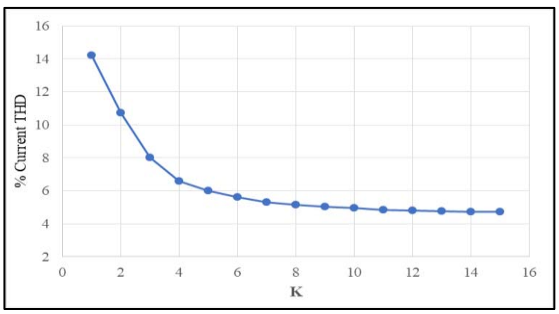

Fig. 13. Percentage change of load current THD with the change of the control circuit gain (K).

almost less than 1%, and has a negligible effect on the overall line voltage shape.

One of the goals of this article is to reduce the cost of the DVR by reducing both the size of the dc-link capacitor and the rating of switching elements. To achieve this goal, the voltage across dc-link capacitor and switches can be limited to low values by using a step-down transformer at the front end of the converter, which could still enable the DVR to compensate for high sag values. The effectiveness of the dc-link regulation and control circuits is assessed for three different parameters, percentage sag, dc-link voltage rating, and dc-link capacitor size, to be able to choose the proper values of capacitor size and voltage rating, as shown in Fig. 14. For example, for a 50% percentage sag in the utility side, the DVR requires a dc voltage level of 7.3 kV when the capacitor size is 5000 μF and, hence, a step-down transformer of almost 30% turns ratio. Decreasing the capacitor size is inversely proportional to the required dc-link voltage to be used and, hence, the voltage stress on switches. Therefore, the set of waveforms shown in Fig. 14 can be used as a setting for the selection of capacitor size for a specifically required percentage sag correction.

Furthermore, the dc-link capacitor voltage V_{dc} should be kept all the times above of the input voltage of the PWM-rectifier $V_{s-\text{rect}}$ to obtain the V_{DVR} magnitude and shape and

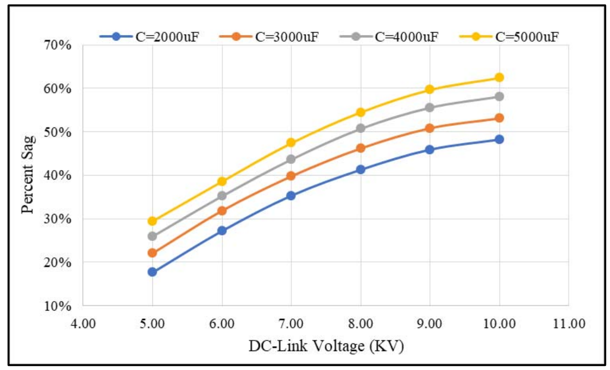

Fig. 14. Percent sag versus dc-link voltage at different capacitor values.

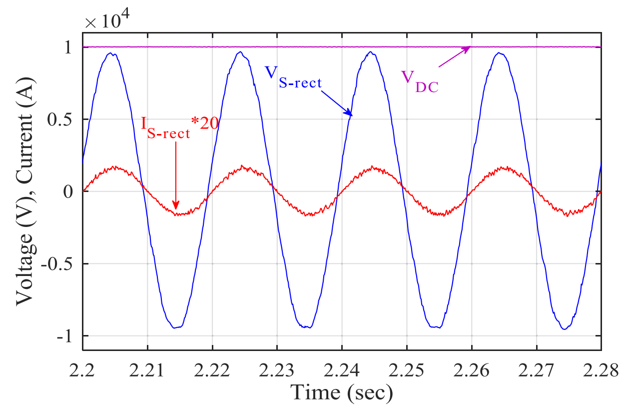

Fig. 15. DC-link capacitor voltage V_{dc}, PWM-rectifier voltage $V_{s-\text{rect}}$, and PWM-rectifier input current $I_{s-\text{rect}}$.

getting a sinusoidal current at the front end of the PWM-rectifier at the same time, as can be observed from the waveforms in Fig. 15.

However, special attention to the PWM-rectifier rating should be considered, especially when the utility grid has some disturbances, as it works as an additional load to the system and may consume considerable power that limits the capability of the wind farm in supporting its main loads and further leads to instability of the system.

The DVR performance is further evaluated when a large nonlinear load, which shares the same bus with the MG, is supplied directly from the utility. As the nonlinear load is drawing a large current that has large harmonic components as well, the voltage at the MG bus V_{MG} is affected both in magnitude and shape, as shown in Fig. 16. However, the DVR could inject a distorted voltage V_{DVR}, which could compensate for voltage sag of almost 45% and decrease the load voltage THD from 22.24% to 2.29%. Furthermore, harmonic's blocking capability of the DVR can be further observed from the source current waveform as its THD is improved to be 8.5%.

B. Mode II: Abnormal Operating Conditions of MG

To assess the DVR response to transients, the power system is subjected to two sudden changes, as shown in Fig. 17 as follows.

1) *Zone-2:* Large load connection (voltage sag).
2) *Zone-4:* Large load disconnection (voltage swell).

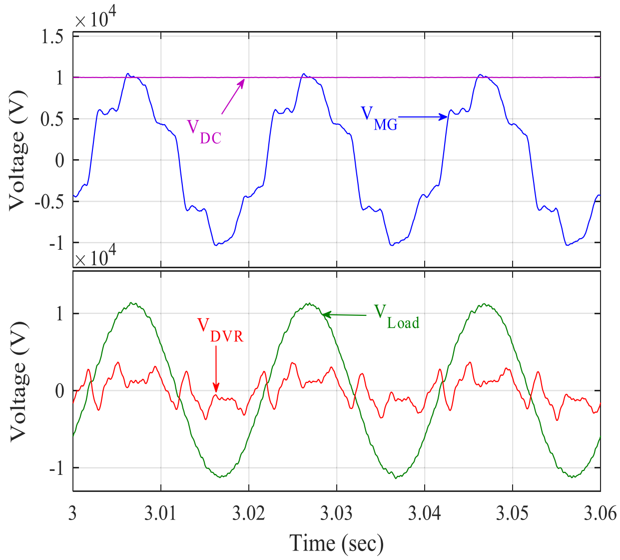

Fig. 16. DVR performance during normal operation using the in-phase control technique with distorted supply voltage.

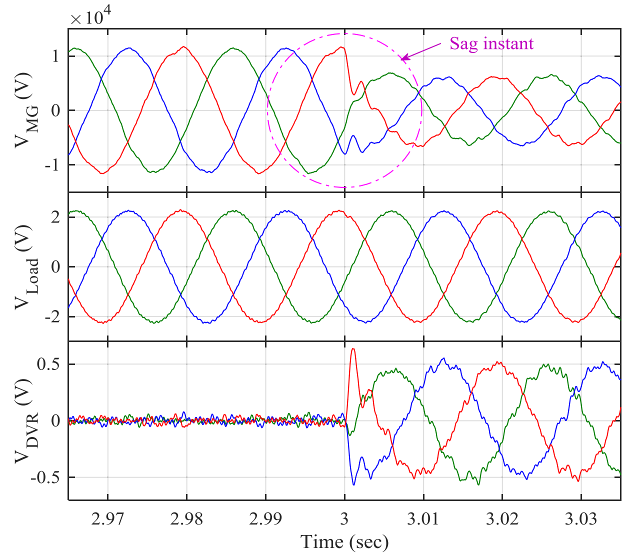

Fig. 18. MG front-end voltage V_{MG}, load voltage V_{Load}, and DVR voltage V_{DVR} at the transition period from Zone-1 to Zone-2 (sag condition).

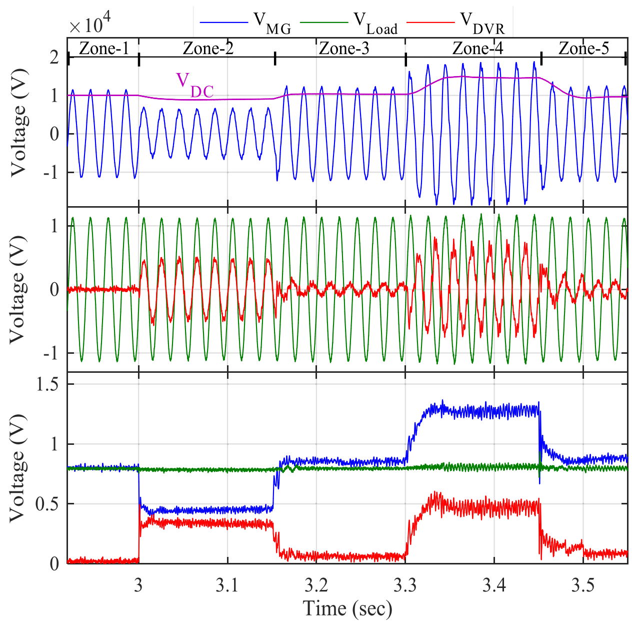

Fig. 17. DVR performance during transients in the utility system using the in-phase control technique.

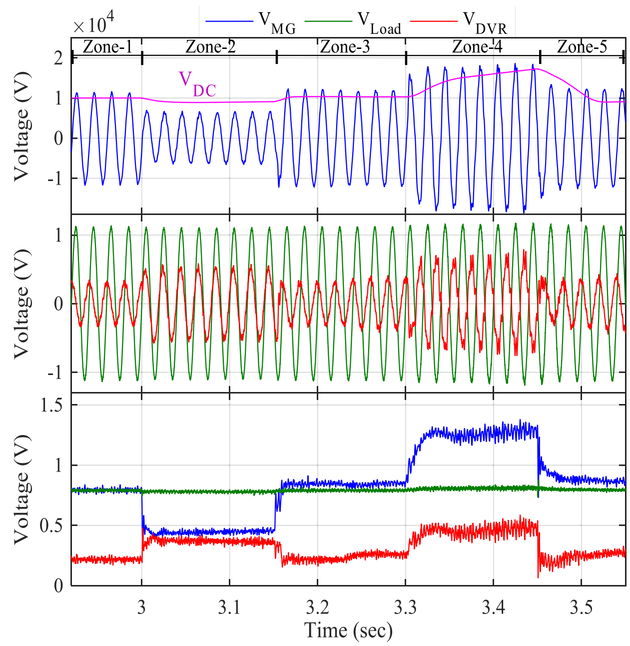

Fig. 19. DVR performance during transients in the utility system using the pre-sag control technique.

The power system is working in its normal condition in Zone-1, and then, the MG faced sudden sag at the begging of Zone-2; as a result, the MG faces a loss of voltage at the common bus, phase jump, and loss of stability, as can be observed from Fig. 18, before the utility is recovered again to its normal condition at the begging of Zone-3. During this transition period, the wind farm's control circuit tries to adapt to these severe and sudden changes by controlling its terminal voltage's parameters, magnitude, phase, and frequency, to maintain its synchronization with utility which is lost for at least two to three cycles. However, the DVR could support and mitigate all the disturbances that happened to the voltage at the common bus and correct the load voltage to its nominal RMS value and follow the same reference phase, as shown in Fig. 18.

The dc-link voltage control circuit could adapt very fast to these changes and keep the dc-link capacitor voltage V_{dc} at all the times above the input voltage of the PWM-rectifier $V_{s-\mathrm{rect}}$ and thus maintain the sinusoidal shape of input current of PWM-rectifier and relieving the power system from the harmonic contents of regular rectifiers. Furthermore, although the PWM-rectifier is working as a load all the times and consuming a considerable power, due to the new control strategy that could decrease its rating and there is no need for load shedding during this transition period.

However, special attention should be considered when designing the control gains of the regulator circuit when using the "in-phase" control technique as the DVR voltage should

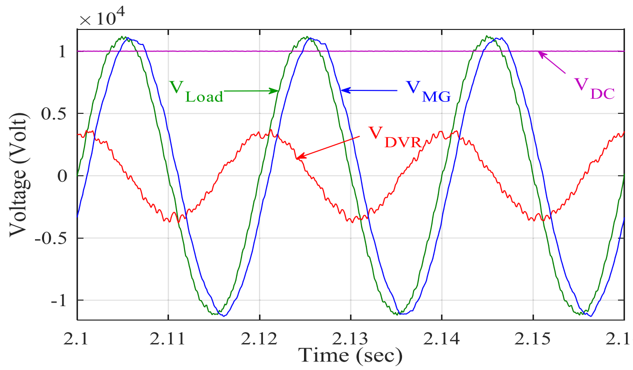

Fig. 20. Load voltage, DVR voltage, and source voltage during normal operation using the pre-phase control technique.

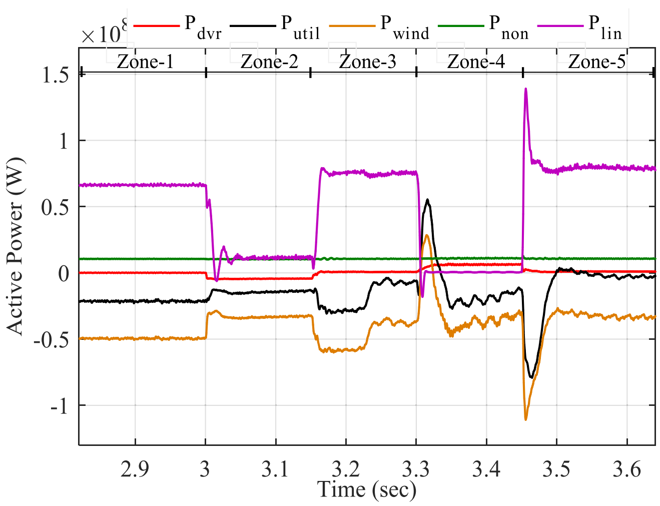

Fig. 21. Active power changes during transients in the utility system using the in-phase control technique.

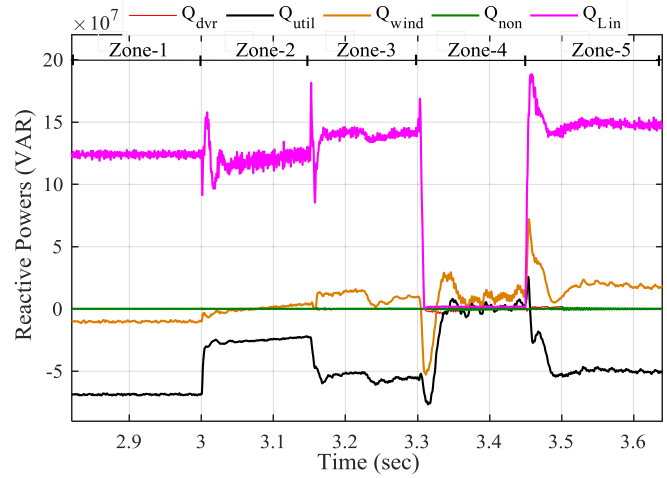

Fig. 22. Reactive power changes during transients in the utility system using the in-phase control technique.

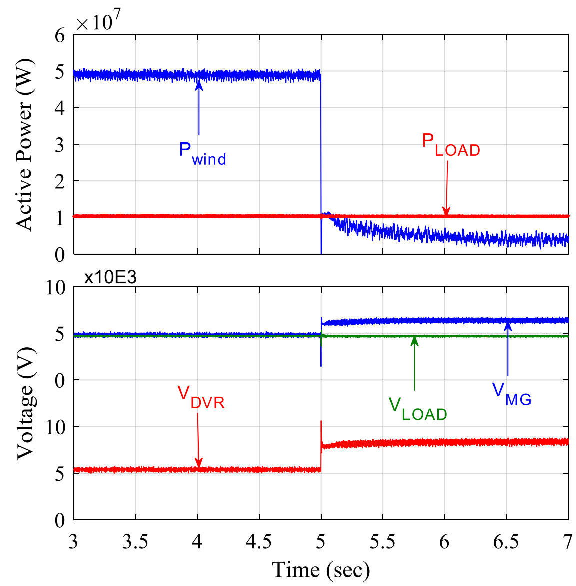

Fig. 23. Effect of change of wind turbine power on the load voltage.

jump very fast from almost zero voltage to almost 50% of the nominal supply voltage, which is not the case when using "pre-sag" compensation technique, shown in Fig. 19, which needs almost 25% of the nominal supply voltage that gives this technique and advantage for power systems that have many nonlinear loads that need fast adaptation to many load variations and transients. Although "pre-sag" technique could be better than "in-phase" technique when dealing with nonlinear loads, it suffers from consistent needs for a higher DVR voltage during the normal mode of operation, as shown in Fig. 20, which increases the stress and losses in the switching elements and hence increasing the wind farm's loading. This may be a crucial point for the MG when working in the islanding mode that needs for most cases to perform load shedding to decrease the instability of the MG.

Furthermore, most interconnection standards require MG to have the ability to handle severe disturbances, commonly known as low voltage ride through (LVRT), which requires that a generator is not allowed to disconnect in the case of a short-term voltage sag in the utility grid [33]. As LVRT capability represents one of the most important technical requirements for wind turbine generators with regard to system reliability, the active and reactive power variations at all the system buses are recorded, as shown in Figs. 21 and 22, respectively, to observe the fast capability of the DVR in keeping the balance of the power system to maintain its reliability. The linear loads that are used in the power systems are all of the constant-impedance types.

It can be observed from Fig. 21 that the DVR can change its active power direction during the sag condition, injecting power in Zone-2, and the swell condition, absorbing power in Zone-4, in a fast manner to keep the system balance and maintain a constant power level for the nonlinear load all the times though the changes in the other power system loads are very severe. It is worth mentioning that the DVR is controlling its input and output powers interchangeably to both maintain the voltage level of the nonlinear load and regulate its dc-link capacitor; as a result, the average contribution of the DVR to the power system is almost zero except for the switching losses in the inverter switches.

Finally, the effect of sudden disconnection of some of the wind turbines on the load voltage is shown in Fig. 23.

Although the wind farm is very close to the load, the DVR could respond in a very fast manner and keep the load voltage at all times and thus can maintain the reliability of the MG to faults from both the utility and within the MG itself.

V. Conclusion

This article proposes a DVR topology that can be used for both voltage compensation and harmonic mitigation. The description and design of the DVR system along with the dc-link capacitor's voltage regulation circuit are provided. Two voltage compensation techniques that are the pre-sag voltage compensation technique and the in-phase voltage compensation technique are adopted to assess the performance of the proposed DVR. The reference current for harmonics mitigation is extracted using the ANC technique. The required power for the regulation of the dc-link capacitor is controlled by a PWM rectifier that is fed from the grid, which has the advantage of drawing a sinusoidal current from the grid.

The validity and effectiveness of the proposed DVR design and dc-link voltage regulation circuit are examined for severe utility disturbances, such as sudden connection and disconnection of large loads and also presence of large nonlinear loads sharing the same bus, which distorts the front end voltage of the MG in both shape and magnitude.

The proposed DVR could prove its capability in controlling its input and output powers interchangeably along with regulating its dc-link capacitor to correct any of the aforementioned abnormalities in the MG front-end voltage in a fast manner, just less than one cycle, and keeping a constant load voltage with low THD, almost 5%.

Furthermore, the DVR could prove its harmonic's blocking capability and decreasing the load current's THD significantly and improving its power factor to almost unity.

However, special attention should be considered when designing the dc-link voltage regulation circuit when using the "in-phase" control technique as the DVR voltage should jump very fast from almost zero voltage to a high voltage value, which is not the case when using "pre-sag" compensation technique that gives later technique and advantage for power systems that have many nonlinear loads that need fast adaptation to many load variations and transients.

Finally, the dc-link capacitor size and voltage can be limited to small values, for example, almost 3000 μF and 7 kV are required for 40% voltage sag but allow proper operation of the DVR scheme, which may decrease the DVR cost significantly.

References

[1] Z. S. AlOtaibi, H. I. Khonkar, A. O. Alamoudi, and S. H. Alqahtani, "Current status and future perspectives for localizing the solar photovoltaic industry in the kingdom of Saudi Arabia," *Energy Transitions*, vol. 4, no. 1, pp. 1–9, Jun. 2020.

[2] W. Kohn, Z. B. Zabinsky, and A. Nerode, "A micro-grid distributed intelligent control and management system," *IEEE Trans. Smart Grid*, vol. 6, no. 6, pp. 2964–2974, Nov. 2015.

[3] I. Askarian, S. Eren, M. Pahlevani, and A. M. Knight, "Digital real-time harmonic estimator for power converters in future micro-grids," *IEEE Trans. Smart Grid*, vol. 9, no. 6, pp. 6398–6407, Nov. 2018.

[4] T. Kandil, "Performance evaluation of anti-islanding protection technique for micro grids," in *Proc. Int. Symp. Smart Electr. Distrib. Syst. Technol. (EDST)*, Sep. 2015, pp. 447–451.

[5] E. Koley, S. K. Shukla, S. Ghosh, and D. K. Mohanta, "Protection scheme for power transmission lines based on SVM and ANN considering the presence of non-linear loads," *IET Gener., Transmiss. Distrib.*, vol. 11, no. 9, pp. 2333–2341, Jun. 2017.

[6] A. A. M. Hassan and T. A. Kandeel, "Effectiveness of frequency relays on networks with multiple distributed generation," *J. Electr. Syst. Inf. Technol.*, vol. 2, no. 1, pp. 75–85, May 2015.

[7] Z. Li, W. Li, and T. Pan, "An optimized compensation strategy of DVR for micro-grid voltage sag," *Protection Control Mod. Power Syst.*, vol. 1, no. 1, pp. 1–8, Dec. 2016.

[8] C. Li, J. Yang, Y. Xu, Y. Wu, and P. Wei, "Classification of voltage sag disturbance sources using fuzzy comprehensive evaluation method," *CIRED-Open Access Proc. J.*, vol. 2017, no. 1, pp. 544–548, Oct. 2017.

[9] N. Ding, W. Cai, J. Suo, J. Wang, and Y. Xu, "Voltage sag disturbance detection based on RMS voltage method," in *Proc. Asia–Pacific Power Energy Eng. Conf.*, Mar. 2009, pp. 1–4.

[10] F. M. Mahdianpoor, R. A. Hooshmand, and M. Ataei, "A new approach to multifunctional dynamic voltage restorer implementation for emergency control in distribution systems," *IEEE Trans. Power Del.*, vol. 26, no. 2, pp. 882–890, Apr. 2011.

[11] A. Ghosh and G. Ledwich, "Compensation of distribution system voltage using DVR," *IEEE Trans. Power Del.*, vol. 17, no. 4, pp. 1030–1036, Oct. 2002.

[12] B. Wang and M. Illindala, "Operation and control of a dynamic voltage restorer using transformer coupled H-bridge converters," *IEEE Trans. Power Electron.*, vol. 21, no. 4, pp. 1053–1061, Jul. 2006.

[13] S. Sasitharan, M. K. Mishra, B. Kalyan Kumar, and V. Jayashankar, "Rating and design issues of DVR injection transformer," in *Proc. 23rd Annu. IEEE Appl. Power Electron. Conf. Expo.*, Austin, TX, USA, Feb. 2008, pp. 449–455.

[14] E. Babaei, M. F. Kangarlu, and M. Sabahi, "Mitigation of voltage disturbances using dynamic voltage restorer based on direct converters," *IEEE Trans. Power Del.*, vol. 25, no. 4, pp. 2676–2683, Oct. 2010.

[15] P. T. Ogunboyo, R. Tiako, and I. E. Davidson, "Effectiveness of dynamic voltage restorer for unbalance voltage mitigation and voltage profile improvement in secondary distribution system," *Can. J. Elect. Comput. Eng.*, vol. 41, no. 2, pp. 105–115, Spring 2018.

[16] P. Kanjiya, B. Singh, A. Chandra, and K. Al-Haddad, "'SRF theory revisited' to control self-supported dynamic voltage restorer (DVR) for unbalanced and nonlinear loads," *IEEE Trans. Ind. Appl.*, vol. 49, no. 5, pp. 2330–2340, Sep./Oct. 2013.

[17] A. G. Ghosh, A. K. Jindal, and A. Joshi, "Design of a capacitor-supported dynamic voltage restorer (DVR) for unbalanced and distorted loads," *IEEE Trans. Power Del.*, vol. 19, no. 1, pp. 405–413, Jan. 2004.

[18] H.-J. Jung, I.-Y. Suh, B.-S. Kim, R.-Y. Kim, S.-Y. Choi, and J.-H. Song, "A study on DVR control for unbalanced voltage compensation," in *Proc. APEC. 17th Annu. IEEE Appl. Power Electron. Conf. Expo.*, vol. 2, Dallas, TX, USA, Mar. 2002, pp. 1068–1073.

[19] K. R. Padiyar, *FACTS Controllers in Power Transmission and Distribution*. New Delhi, India: New Age International (P) Limited, 2007.

[20] A. Ghosh and G. Ledwich, "Structures and control of a dynamic voltage regulator (DVR)," in *Proc. IEEE Power Eng. Soc. Winter Meeting. Conf.*, vol. 3, Columbus, OH, USA, Jan./Feb. 2001, pp. 1027–1032.

[21] M. Pradhan and M. K. Mishra, "Dual $P-Q$ theory based energy-optimized dynamic voltage restorer for power quality improvement in a distribution system," *IEEE Trans. Ind. Electron.*, vol. 66, no. 4, pp. 2946–2955, Apr. 2019.

[22] S. Guo and D. Liu, "Proportional-resonant based high-performance control strategy for voltage-quality in dynamic voltage restorer system," in *Proc. 2nd Int. Symp. Power Electron. Distrib. Gener. Syst.*, Jun. 2010, pp. 721–726.

[23] V. K. Remya, P. Parthiban, V. Ansal, and B. Chitti Babu, "Dynamic Voltage Restorer (DVR)–A Review," *J. Green Eng.*, vol. 8, no. 4, pp. 519–572, Oct. 2011.

[24] C. Weiji, C. Wenhong, M. Xiaojun, C. Jianye, W. Zhonghong, and H. Yingduo, "An adaptive noise canceling theory based single-phase shunt active power filter," in *Proc. Power Convers. Conf. (PCC)*, vol. 1, Aug. 1997, pp. 191–196.

[25] A. A. Helal and M. H. Saied, "Dynamic voltage restorer adopting 150° conduction angle VSI," in *Proc. IEEE Canada Electr. Power Conf.*, Vancouver, BC, Canada, Oct. 2008, pp. 1–6.

[26] F. A. L. Jowder, "Design and analysis of dynamic voltage restorer for deep voltage sag and harmonic compensation," *IET Gener., Transmiss. Distrib.*, vol. 3, no. 6, pp. 547–560, Jun. 2009.

[27] N. Mohan, T. M. Undeland and W. P. Robbins, *Power Electronics: Converters, Applications and Design*. Hoboken, NJ, USA: Wiley, 1989, pp. 425–426.

[28] S. Kwak and H. A. Toliyat, "Design and rating comparisons of PWM voltage source rectifiers and active power filters for AC drives with unity power factor," *IEEE Trans. Power Electron.*, vol. 20, no. 5, pp. 1133–1142, Sep. 2005.

[29] D. M. Vilathgamuwa, A. A. D. R. Perera, and S. S. Choi, "Voltage sag compensation with energy optimized dynamic voltage restorer," *IEEE Trans. Power Del.*, vol. 18, no. 3, pp. 928–936, Jul. 2003.

[30] H. Kim, J.-H. Kim, and S.-K. Sul, "A design consideration of output filters for dynamic voltage restorers," in *Proc. IEEE 35th Annu. Power Electron. Spec. Conf.*, Jun. 2004, pp. 4268–4272.

[31] S. S. Choi, J. D. Li, and D. M. Vilathgamuwa, "A generalized voltage compensation strategy for mitigating the impacts of voltage sags/swells," *IEEE Trans. Power Del.*, vol. 20, no. 3, pp. 2289–2297, Jul. 2005.

[32] C.-S. Lam, M.-C. Wong, and Y.-D. Han, "Voltage swell and overvoltage compensation with unidirectional power flow controlled dynamic voltage restorer," *IEEE Trans. Power Del.*, vol. 23, no. 4, pp. 2513–2521, Oct. 2008.

[33] A. Benali, M. Khiat, T. Allaoui, and M. Denai, "Power quality improvement and low voltage ride through capability in hybrid wind-PV farms grid-connected using dynamic voltage restorer," *IEEE Access*, vol. 6, pp. 68634–68648, 2018.

Tarek Kandil received the B.Sc. and M.Sc. degrees from Cairo University, Cairo, Egypt, in 1993 and 1999, respectively, and the Ph.D. degree from the University of Alberta, Edmonton, AB, Canada, in 2004.

He was working as an Associate Professor with Alazhar University, Cairo, from 2011 to 2014. He is currently working with Jouf University, Sakakah, Saudi Arabia. His research interests include power quality, active filters, distributed generation, and microgrid protection.

Mohamed Adel Ahmed received the B.Sc. and M.Sc. degrees from Benha University, Benha, Egypt, in 2000 and 2006, respectively, and the Ph.D. degree in electrical engineering from Cairo University, Cairo, Egypt, in 2011.

From 2002 to 2014, he was with the Department of Electrical Engineering and Technology, Faculty of Engineering, Benha University. Since 2014, he has been an Assistant Professor with the Department of Electrical Engineering, Jouf University, Sakakah, Saudi Arabia. His research interests include machine drives, power quality, active filters, distributed generation, and microgrids.